THESIS FOR THE DEGREE OF LICENTIATE OF ENGINEERING IN SOLID AND STRUCTURAL MECHANICS

# Robust analysis of delaminating composites using adaptive isogeometric shell elements


Elias Börjesson





Department of Industrial and Material Science
Chalmers University of Technology
Gothenburg, Sweden, 2022

**Robust analysis of delaminating composites using adaptive isogeometric shell elements**

Elias Börjesson



Technical Report No. IMS-2022-3
This thesis has been prepared using LaTeX.

Department of Industrial and Material Science
Chalmers University of Technology
SE-412 96 Gothenburg, Sweden
Phone: +46 (0)31 772 1000
`www.chalmers.se`

Cover: Element configuration and interface damage for a cantilever beam with two initial delaminations, and that is subjected to an edge load.

Printed by Chalmers Reproservice
Gothenburg, Sweden, April 2022

# Abstract

Fibre reinforced composites are considered to be one of the material categories that offer the best possibilities to create efficient lightweight designs. Many companies in the transport sector therefore work towards increasing the amount of fibre composites in their products, in an attempt to lower the fuel consumption of their vehicles. However, from the perspective of simulation-driven design, an increased use of composite materials is accompanied with new modelling challenges. In this thesis, two such challenges have been considered.

The first challenge concerns the often computationally demanding models needed to simulate delamination in fibre composites. The heterogeneous through-thickness nature of fibre composites necessitates a very fine through-thickness discretisation in order to capture the delamination process, which leads to very long (or even infeasible) simulation times. The second challenge addressed in this thesis is related to the difficulties arising when simulating the post-failure response of fibre composites. Specifically, in quasi-static simulations, the brittle material interfaces of layered fibre composites can lead to sudden failure, which standard incremental Newton-Raphson solvers are not able to trace.

To address these problems, two new computational tools have been developed that can aid the design process of fibre reinforced composites. Firstly, in Paper A, an adaptive isogeometric shell element has been developed, that can refine its through-thickness kinematics as delamination propagates. Consequently, only the lowest level of detail needed to capture delamination is included in the model, which improves efficiency. To address the second issue, a dissipation based path-following solver has been developed in Paper B, which is able to robustly trace the equilibrium path of the post-peak response in quasi-static simulations.

Both Paper A and Paper B shows that the developed adaptive isogeometric shell element and the dissipation based path-following solver can be combined to robustly and efficiently simulate composite structures with brittle delamination behaviour. Consequently, it is shown that the computational tools developed in this thesis can be used to aid the design process of fibre reinforced structures.

**Keywords:** Isogeometric analysis, adaptive, delamination, path-following.

## Acknowledgments

I would like to start by thanking my supervisors Martin Fagerström and Joris Remmers for the excellent guidance you have given me in the first 2.3 years of my PhD thesis. Working with you has been incredibly fun and rewarding, and I am looking forward to our continued collaboration in the second half of my thesis. I would also like to thank all my colleagues at the division for making the office such a fun place to work at. Going to work would not be as easy without you. A big thanks to Fredrik, Kim, Kristoffer and the other developers of the finite element toolbox "Ferrite.jl", for our collaborations and code-sharing, which have made all the coding and implementations in my thesis possible. Finally, a special thanks to Johanna and Jim for "taking me under their wings", and for always having an open door to their offices so I can disturb them when I want :).

## Acronyms

| | |
|---|---|
| IGA: | Isogeometric Analysis |
| CAD: | Computer Aided Design |
| CAE: | Computer Aided Engineering |
| LW: | Layer-Wise |
| ESL: | Equivalent Single-Layer |

# List of Publications

This thesis is based on the following publications:

[A] **Elias Börjesson**, Joris J.C. Remmers, Martin Fagerström, "An adaptive isogeometric shell element for the prediction of initiation and growth of multiple delaminations in curved composite structures". *Computers and Structures,* Vol. 260, no. 10, Feb. 2022, 0045-7949.

[B] **Elias Börjesson**, Joris J.C. Remmers, Martin Fagerström, "A generalised path-following solver for robust analysis of material failure". *Submitted for publication.*

# Contents

**Abstract** i

**Acknowledgements** iii

**Acronyms** iii

**List of Papers** v

## I Overview 1

**1 Introduction** 3
- 1.1 Failure mechanisms in fibre composites . . . . . . . . . . . . . . 4
- 1.2 Current composite modelling methods . . . . . . . . . . . . . . 6
- 1.3 Research scope . . . . . . . . . . . . . . . . . . . . . . . . . . . 7

**2 Adaptive isogeometric shell element** 9
- 2.1 Introduction to IGA . . . . . . . . . . . . . . . . . . . . . . . . 10
  - 2.1.1 B-Splines functions . . . . . . . . . . . . . . . . . . . . . 11
  - 2.1.2 Knot insertion . . . . . . . . . . . . . . . . . . . . . . . 14
- 2.2 Adaptive isogeometric shell element . . . . . . . . . . . . . . . 14
  - 2.2.1 Shell kinematics . . . . . . . . . . . . . . . . . . . . . . 15

2.2.2 Adaptive refinement of through thickness kinematics . . 17
2.2.3 Stress recovery . . . . . . . . . . . . . . . . . . . . . . . . 19
2.2.4 Refinement criteria . . . . . . . . . . . . . . . . . . . . . . 21

**3 Dissipation based path-following solver 23**
3.1 Fundamentals of path-following solvers . . . . . . . . . . . . . . 25
3.2 Path-following constraints . . . . . . . . . . . . . . . . . . . . . 26
3.3 Our dissipation based path-following constraint . . . . . . . . . 27
3.4 Algorithmic aspects . . . . . . . . . . . . . . . . . . . . . . . . . 28
3.4.1 Elastic regimes of the equilibrium curve . . . . . . . . . 28
3.4.2 Adaptive adjustment of the path-following parameter . 29

**4 Discussion and concluding remarks 31**

**5 Future work 35**

**References 37**

**II Papers 41**

**A An adaptive isogeometric shell element for the prediction of initiation and growth of multiple delaminations in curved composite structures A1**

**B A generalised path-following solver for robust analysis of material failure B1**

# Part I

# Overview

# CHAPTER 1

# Introduction

The ability to design lightweight structures is of great importance in many industries, especially in the transport sector, where the weight of the vehicle is directly related to its fuel consumption. A group of materials that is beneficial for lightweight design are fibre reinforced composites, where fibres (e.g. carbon, glass, kevlar) are embedded inside a polymer matrix (e.g. epoxy). Their properties and internal structure are favourable in (at least) two ways. Firstly, fibre composites possess good stiffness- and strength-to-weight ratios, and secondly, the orientation and angles of the fibres can be tailored such that optimal properties are obtained for the specific application.

For these reasons, the aero industry has long been an industry where the increased production cost, typically associated with fibre composites, has been easily justified. As an example, the airframe of the Boeing 787 (that was started to be produced 2007), is composed of approximately 50% carbon fibre reinforced plastics and other composites (by weight) [1]. However, the adaptation of composites in other industries, for example the automotive industry, has been slower, and can mainly be found in some low-series production cars.

There are multiple reasons why fibre composites are not the predominately used material in industries where lightweight structures are important. One big reason is that the cost of fibre composites (raw material and manufacturing) is typically much higher than for traditional materials such as steel and aluminium. As an example, Heuss et al. [2] estimated that manufacturing an automotive fender in fibre composite material was 570% more expensive than the steel counterpart (although also 50% lighter). Other issues that impede the use of fibre composites are challenges in manufacturability, quality assurance, recycling, experience etc.

Another important challenge accompanied by increased use of fibre composites, which has been the focus of this thesis, is the increased complexity in computationally predicting the initiation and propagation of damage in the material. The heterogeneous cross-sectional material properties of fibre composites give rise to a number of complex failure modes, which require very detailed (and thereby computationally heavy) models to be captured. Since Computer Aided Engineering (CAE) has a central role in the product development process in modern industries, with demand for short simulation times, it is therefore difficult to properly evaluate the possible benefits obtained by using fibre composites in the structures. New and more efficient numerical tools would therefore facilitate the possibility for introducing more fibre composite materials in the future vehicles being developed.

Another challenge associated with modelling the failure of fibre composites is that they can typically cause very brittle failure events, which makes it difficult to use standard solution methods to simulate the post-failure response. As a result, it is not only important to develop new material and failure models, but to also develop robust solvers that can simulate the full failure event of said models.

## 1.1 Failure mechanisms in fibre composites

Figure 1.1 shows a corrugated NCF composite panel subjected to crushing (figure taken from the works of Grauers [3]). From this figure it is evident that fibre composites are characterised by many complex and competing failure mechanisms, for example delamination, fibre kinking, tensile fibre failure and matrix cracking. These failure mechanisms can occur simultaneously or in sequence, and numerical tools that aim to model these phenomenon should therefore be capable of accurately capturing the interplay between several progressive failure modes.

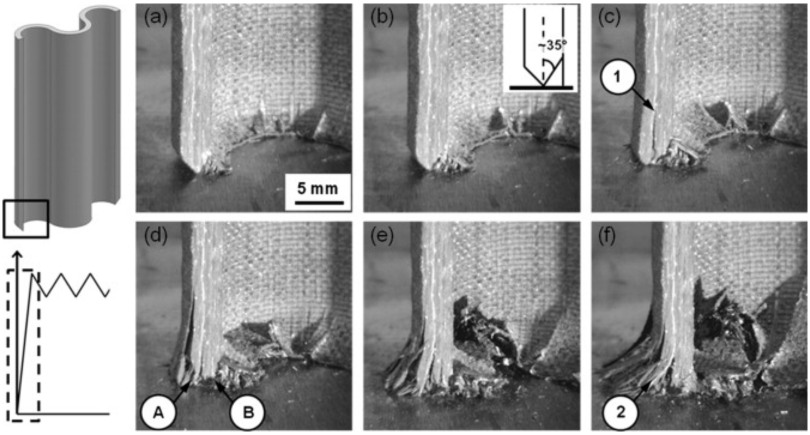


**Figure 1.1:** Laminated fibre composite subjected to crushing. Failure mechanisms: bending of plies (A), compressive failure (B), delamination in mode I (1), and delamination in mixed mode (2). *From Grauers (2013) [3]. Reprinted with permission.*

For many applications, the interplay of modes is strongly affected by the amount of delamination. This is again evident from the laminate subjected to progressive crushing in Figure 1.1. A central Mode I delamination was initiated early in the crushing process, which separated the laminates into two parts, where one part tended to fail predominately in bending, whereas the lower part tended to fail more in compression modes. Similar results was also found by Hull [4]. From these experimental results it is obvious that, in order to get good predictability in simulations, delamination needs to be accounted for.

Most of the underlying damage mechanisms mentioned above are initiated in a multi-axial stress state. Thus, for an accurate component design against damage initiation, it is important to capture the complete three-dimensional stress state. This means that often a fine resolution of the through-thickness direction (together with sophisticated damage models) is needed. Furthermore, delamination adds to this complexity, since it is fundamentally a discrete failure which separates the composite laminate into new geometrical parts.

## 1.2 Current composite modelling methods

Current techniques used for modelling fibre reinforced composites can broadly be divided into two categories. In the first category, the entire layup of the composite is modelled as a single element. These models are therefore referred to as Equivalent Single-Layer models (ESL), see Figure 1.2a for an illustration. The ESL modelling approach is an extension of traditional simulation methods for homogeneous material such as metals, where each element has three rotational and three displacement degrees of freedoms per node. As such, ESL models are considered to be computationally efficient, however, they lack the capabilities to capture the kinematics of many failure modes. In order to model some of the complex failure modes with ESL models, phenomenological material models can be used, see e.g Feraboli et al. [5]. However since these lack the connection with physical reality, extensive testing and validation is required for each specific material lay-up. Nevertheless, ESL models are often used due to their efficiency, especially in crash simulations where they become the only feasible option.

An alternative modelling approach that enables more physically accurate simulations, are Layer-Wise (LW) models, see e.g. Costa et al. [6]. As opposed to ESL models, LW models resolve the through-thickness directions by modelling each layer of the composite with one or more solid elements, see Figure 1.2b. Modelling each layer enables a better representation of the kinematics in the delamination process, by also adding cohesive zone elements between each layer. Furthermore, it is also possible to include damage models for simulating failure mechanisms such as fibre kinking and matrix cracking via continuum damage models [7], which means that LW models can in general predict the complete failure process. However, a major drawback with LW models is the huge amount of computational resources required to use them, especially when the number of plies in the composite is large.

In an attempt to address the computationally heavy models obtained with the LW models, several authors have proposed adaptive modelling approaches which aim to combine ESL and LW elements, see e.g. [8]–[11]. The common idea in these adaptive methods is to initialise the simulation with only ESL based elements, and then adaptively refine the elements through-thickness discretisation when damage propagation is detected. In this way, the model can remain largely efficient by only using detailed LW discretisation where it is needed.

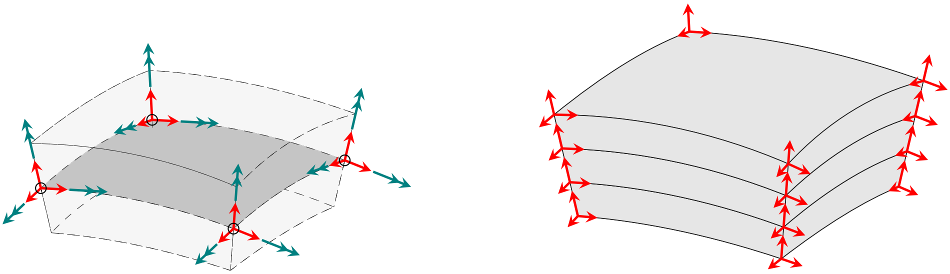

**(a)** Equivalent Single-Layer

**(b)** Layer-Wise model

**Figure 1.2:** Illustration of two modelling approaches for fibre composites. Red arrows symbolise displacement degrees of freedom and green arrows symbolise rotational degrees of freedom.

## 1.3 Research scope

The complex failure process of fibre reinforced composites makes it difficult to efficiently and robustly evaluate them for use in lightweight designs. Therefore, the first research goal of this thesis has been to develop an isogeometric shell model that can adaptively refine its discretisation at arbitrary interfaces through the thickness, with the aim of combining the efficiency of ESL models and kinematical accuracy of LW models. Furthermore, a stress recovery method for arbitrarily curved geometries has been included in the adaptive modelling framework, for improved stress prediction in ESL type elements and to predict the initiation of new delamination zones. Note that as a first step, no adaptive capabilities in the in-plane direction have been developed.

The adaptive continuum shell element is formulated in an isogeometric framework, to explore the benefits of having *(i)* exact representation of the geometry, *(ii)* less locking behaviour in shell elements, and *(iii)* continuity of the stress and strain field. The first and third point will especially be advantageous for the stress recovery method.

The second research goal has been to improve the robustness of quasi-static solution procedures used for analysing the failure behaviour of fibre reinforced composites. This has been addressed by developing a dissipation based path-following solver.

# CHAPTER 2

# Adaptive isogeometric shell element

To address the issues related to layer-wise and equivalent single-layer models, I have in this thesis developed an adaptive continuum-shell element (Paper A). My work is a continuation of the work made by Hosseini et al. [12], and then later extended by Adams et al. [11], where an adaptive continuum shell element within an isogeometric framework was proposed.

The main idea with an adaptive model is to initiate the simulation with a coarse discretisation (and/or computationally efficient element formulation), and then progressively refine the discretisation as damage starts to form and propagate, thereby only using the lowest level of detail required for the simulation. The use of adaptive finite element models for analysing fibre reinforced composites is not a new idea, and several different but related approaches have already been proposed, see for example [8]–[10]. In this thesis, however, the current adaptive shell model is developed in an isogeometric framework, which comes with some interesting advantages. These advantages will be outlined in this chapter.

The main parts of the adaptive isogeometric shell element can be summarised as follows:

- A standard shell formulation representing the undeformed and deformed configurations, described with isogeometric basis functions and curvelinear coordinates.

- An isogeometric continuum-shell formulation for describing the displacement field. This isogeometric framework allows for flexible control of the out-of-plane discretisation.
- Utilisation of the stress recovery method for improving the prediction of the transverse stresses in elements with coarse through-thickness discretisation. The stress-recovery method is formulated for arbitrarily curved geometries.
- Criteria based on the stress- and damage-state of the elements for deciding when the adaptive model should be refined.

These four main parts of the element will be described in more detail in the following subsections. However, first an introduction to isogeometric analysis will be given.

## 2.1 Introduction to IGA

IGA was first proposed in 2005 with the goal of reducing the considerable amount of time spent on meshing and creation of finite element models for industrial applications [13]. IGA facilitates a reduction in time spent on model creation by unifying Computer Aided Design (CAD) with computer aided engineering (CAE). What makes the unification of these two fields possible, are their respective similarities in the geometrical parametrisation of surfaces and volumes. CAD geometries and surfaces, much like in FE-models, are represented by a linear combination of control points (nodes) and basis functions. The main idea with isogeometric analysis is then to utilise these CAD basis functions directly, and thereby circumvent the sometimes very cumbersome work of transforming the CAD model to a finite element model.

The basis functions used in modern CAD software belong to a family of curves called spline functions. These spline functions possess some interesting properties compared to the standard Lagrange polynomials used in FEM. One important property, is that splines are (at least) $C^1$ continuous over element boundaries, whereas Lagrange polynomials are always $C^0$ continuous, see Figure 2.1 for a visual comparison of the different basis functions in a domain.

A benefit from this higher order continuity is that they lead to a higher convergence rate (in terms of the number of degrees of freedom in the model). Furthermore, higher order continuity also leads to continuity of the stress and strain fields within the IGA-patch (i.e. part of the domain). Another benefit is that spline functions can be constructed as rational polynomials, which means that they can be used to represent conical sections (for example circles) exactly. This means that IGA based models do not introduce any geometrical approximation, since the domain is represented exactly.

Isogeometric analysis does however face some challenges that currently prevent it from being the go-to design tool in the industry. Some examples of these challenges are; connection of IGA-patches, how to handle trimmed surfaces, local refinement, to name a few. I will not attempt to explain these issues in this thesis, but the interested reader can see the works of e.g. Bazilevs et al. [14] or Leidinger et al. [15]. These challenges however, have been active research topics within the IGA community from the start, and promising improvements in all these topics have been made. Furthermore, there now exists many papers demonstrating an isogeometric workflow [15] (i.e. cad geometries used directly for analysis), and industry CAE software developers has started to implement IGA functionality in to their solvers, see for example in LS-DYNA [16].

In the next section, the fundamentals of isogeometric basis functions (B-spline basis functions) will be introduced.

### 2.1.1 B-Splines functions

The underlying basis functions used in CAD geometries and isogeometric analysis are so-called B-spline basis functions. They are generated using the Cox-de Boor recursive algorithm:

$$N_{i,p}(\xi) = \frac{\xi - \xi_i}{\xi_{i+p} - \xi_i} N_{i,p-1}(\xi) + \frac{\xi_{i+p+1} - \xi}{\xi_{i+p+1} - \xi_{i+1}} N_{i+1,p-1}(\xi) \tag{2.1}$$

where

$$N_{i,0}(\xi) = \begin{cases} 1 & \xi_i \leq \xi \leq \xi_{i+1} \\ 0 & \text{otherwise} \end{cases} \tag{2.2}$$

In the above definition, $N_{i,p}(\xi)$ are B-spline basis functions, and $p$ and $n$

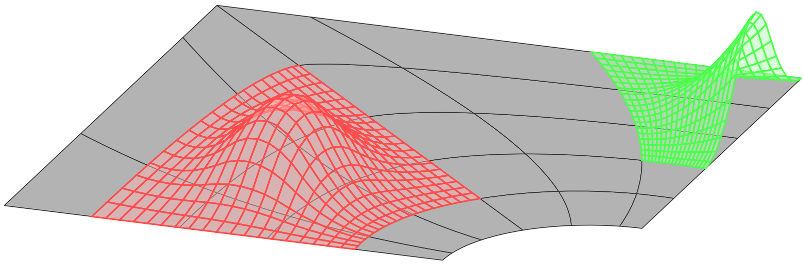

**(a)** IGA with spline functions.

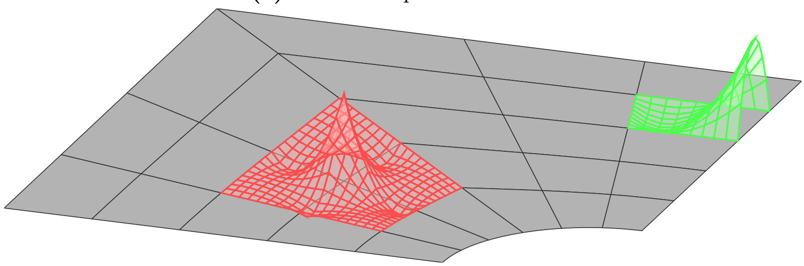

**(b)** FEM with Lagrange polynomials.

**Figure 2.1:** Comparison of a IGA and FEM discretisation of a plate with a hole. The basis functions from the IGA domain are $C^1$ continuous over element boundaries.

are the order and number of basis functions, respectively. The values $\xi_i$ are so-called knot values, which are collected in a non-decreasing knot vector, $\boldsymbol{\Xi}$:

$$\boldsymbol{\Xi} = [\xi_1, \xi_2, \ldots, \xi_{n+p+1}]. \tag{2.3}$$

In Figure 2.2a, seven second order ($p = 2$) basis functions constructed from the knot vector $\boldsymbol{\Xi} = [0, 0, 0, 1, 2, 3, 4, 5, 5, 5]$ are shown (note that the first and last knot values have been repeated in order to an obtain interpolating ends).

The knot vector and knot values have important roles for the construction of the basis functions, as they can be used to control the number of elements in the IGA discretisation. Furthermore, the knot vector can also be used to control the continuity of the basis functions, as will be shown in Subsection 2.1.2.

Geometrical B-spline curves, $C(\xi)$, can be constructed as a linear combination of B-spline basis functions:

$$C(\xi) = \sum_{i=1}^{n} N_{i,p}(\xi)\hat{\boldsymbol{x}}_i \tag{2.4}$$

where $\hat{\boldsymbol{x}}_i$ are control points (as comparted to nodal coordinates in the finite element method). As en example, Figure 2.2b shows a curve defined by the basis functions in Figure 2.2a and 7 control points. Surfaces and volumes can be constructed in a similar fashion via a tensor product of multiple B-spline basis functions in different parametric direction.

The most common type of spline function used in CAD software is Non-Uniform Rational B-splines (NURBS). They have become the standard due to their ability to represent conical sections (e.g. circles) exactly (which is not possible with polynomial functions such as B-splines). NURBS basis functions, $R_{i,p}$, are associated with an weight, $w_i > 0$, and are constructed as:

$$R_{i,p} = \frac{N_{i,p}(\xi)w_i}{W(\xi)}, \quad \text{with} \quad W(\xi) = \sum_{i=1}^{n} N_{i,p}(\xi)w_i \tag{2.5}$$

NURBS functions can then be combined in a similar manner as in Equation (2.4), to represent curves (and surfaces and volumes).

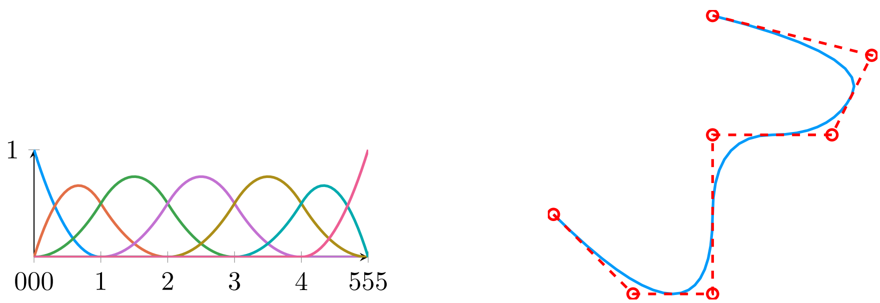


**(a)** B-spline basis.

**(b)** B-spline curve.

**Figure 2.2:** Illustration of B-Spline basis functions and a B-spline curve. The control points in (b) are illustrated as red circles.

### 2.1.2 Knot insertion

Knot-insertion is a fundamental technique used in IGA to refine the discretisation of the domain. It is performed by inserting new knots into the knot-vector $\mathbf{\Xi}$. A important feature of knot-insertion is that it can be performed without altering the original geometry of the domain. In order to see this, consider a knot vector where a new knot has been inserted at $\bar{\xi} \in [\xi_k, \xi_{k+1}]$. The new set of $m = n + 1$ control points, $\left\{\bar{\boldsymbol{P}}_A\right\}_{A=1}^{m}$, are then formed as a linear combination of the original points $\{\boldsymbol{P}_A\}_{A=1}^{n}$:

$$\bar{\boldsymbol{P}}_A = \begin{cases} \boldsymbol{P}_1, & A = 1 \\ \alpha_A \boldsymbol{P}_A + (1 - \alpha_A)\boldsymbol{P}_{A-1}, & 1 < A < m \\ \boldsymbol{P}_n & A = m \end{cases} \tag{2.6}$$

where

$$\alpha_A = \begin{cases} 1, & 1 \leq A = 1 \leq k - p \\ \frac{\bar{\xi} - \xi_A}{\xi_{A+p} - \xi_A}, & k - p + 1 \leq A \leq k \\ 0 & A \geq k + 1 \end{cases} \tag{2.7}$$

As an example, Figure 2.3a shows an enriched set of basis functions when a knot $\xi = 3.5$ has been inserted into the original knot vector $\mathbf{\Xi} = [0, 0, 0, 1, 2, 3, 4, 5, 5, 5]$ from Figure 2.2a. Figure 2.3b shows the corresponding spline curve with the new set of control points, but note that the geometry of the curve is left unchanged.

Knot-insertion can also be used to control the continuity of the basis-functions. This is achieved by increasing the multiplicity of a knot value in the knot vector. For example, continuing with the set of B-spline basis function in shown Figure 2.2a, Figure 2.4a illustrate how the continuity of a basis function is reduced to $C^0$ continuity, when the knot value $\xi = 4$ is repeated. This feature will be used for flexible control the out-of-plane discretisation in the proposed shell element.

## 2.2 Adaptive isogeometric shell element

As mentioned in the introduction of this chapter, the adaptive shell element is developed in an isogeometric framework, which means the underlying

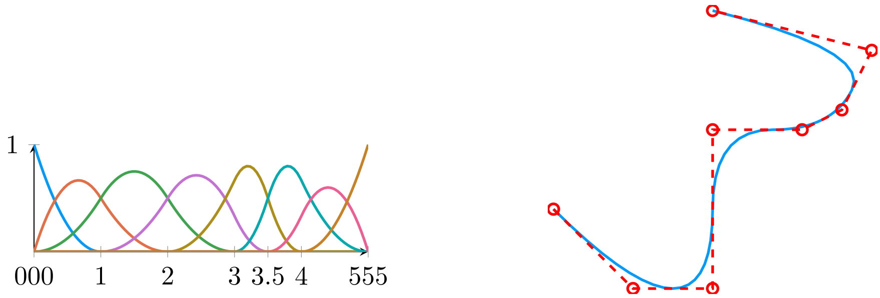


**(a)** Enriched B-spline basis. **(b)** Resulting B-spline curve

**Figure 2.3:** The basis functions and resulting B-spline curve after a knot has been inserted at $\xi = 3.5$.

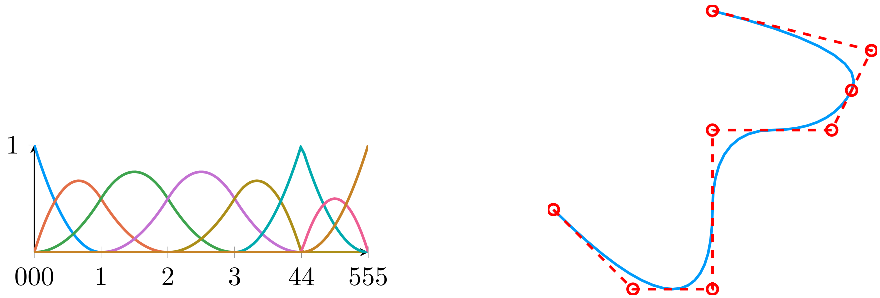


**(a)** B-spline basis. **(b)** Resulting B-spline curve.

**Figure 2.4:** The basis functions and resulting B-spline curve after a knot has been inserted at $\xi = 4$.

parametrisation of the geometry is described with spline functions. On top of this, the adaptive shell formulation has been built. In this section, the four main parts (introduced in the beginning of this chapter) of the shell element is described.

### 2.2.1 Shell kinematics

The underlying geometric and kinematic description of the element is based on a standard formulation for shells. The mid-surfaces of the undeformed and deformed configurations, seen in Figure 2.5, are defined by a curve-linear

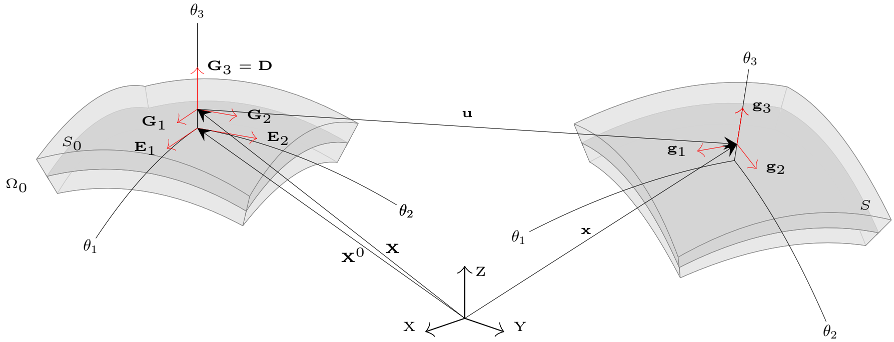


**Figure 2.5:** Kinematics of the continuum shell in the undeformed and deformed configuration.

coordinate system with coordinates $\theta_1$, $\theta_2$ and $\theta_3$ (where $\theta_3$ is the coordinate in the thickness direction). A material point in the undeformed configuration, $\boldsymbol{X}(\theta_1, \theta_2, \theta_3)$, is computed as:

$$\boldsymbol{X}(\theta_1, \theta_2, \theta_3) = \boldsymbol{X}^0(\theta_1, \theta_2) + \theta_3 \frac{t}{2} \mathbf{D}(\theta_1, \theta_2), \quad -1 \leq \theta_3 \leq 1 \tag{2.8}$$

where $t$ is the thickness of the shell, $\boldsymbol{X}^0$ is the position corresponding to a point at the mid-surface of the shell and $\boldsymbol{D}$ is a unit vector normal to the surface. A material point in the deformed configuration, $\mathbf{x}(\theta_1, \theta_2, \theta_3)$, can be expressed as:

$$\boldsymbol{x}(\theta_1, \theta_2, \theta_3) = \boldsymbol{X}(\theta_1, \theta_2, \theta_3) + \boldsymbol{u}(\theta_1, \theta_2, \theta_3) \tag{2.9}$$

where $\boldsymbol{u}$ is the displacement field. The kinematic description of the displacement field may be chosen in multiple ways, for example using the Kirchhoff-Love or Mindilin-Reissner assumptions, however in this thesis a continuum-shell representation has been chosen.

For a more detailed description of the full shell formulation, the reader is referred to Hosseini et al. [12].

### 2.2.2 Adaptive refinement of through thickness kinematics

The displacement field $\boldsymbol{u}$ introduced in Equation (2.9) is described using a continuum-shell representation:

$$\boldsymbol{u}(\theta_1, \theta_2, \theta_3) = \sum_{I=1}^{N_{cp}} N(\theta_1, \theta_2, \theta_3)\boldsymbol{a}_I, \tag{2.10}$$

where $N_{\text{cp}}$ are the number of control points, $\boldsymbol{a}_I$ are displacement degrees of freedom, and $N(\theta_1, \theta_2, \theta_3)$ are tri-variate basis functions. The basis functions has been constructed as a combination of bi-variate in-plane NURBS basis functions $H(\theta_1, \theta_2)$, and uni-variate out-of-plane B-spline functions $S(\theta_3)$:

$$\begin{aligned} N_I = H_i(\theta_1, \theta_2)S_j(\theta_3), \\ i = [1, \ldots, k], \\ j = [1, \ldots, l], \end{aligned} \tag{2.11}$$

where $k$ and $l$ are the number of control-points in the in-plane and out-of-plane directions, respectively. This split of the in-plane and out-of-plane directions allows for individual control of the discretisation level and kinematics of each respective direction.

As an illustration, consider a shell element consisting of three layers, where the out-of-plane direction is discretised by second order ($p = 2$) B-spline basis functions. We will now consider three different configurations for which the control-points of the element can take; *lumped*, *layered* and *discontinuous*. These configurations are described below.

***lumped***

The coarsest possible discretisation in a control point is obtained with the knot vector $\boldsymbol{\Xi} = [-1, -1, -1, 1, 1, 1]$, and can be seen in Figure 2.6a. A control point in this configuration is said to be in a *lumped* state, because all layers are lumped into one element through the thickness. Note that this state resembles an ESL model, and as such, is relatively computationally efficient. Due to the coarse out-of-plane resolution, an element in this configuration can not predict the transverse stresses normal to the mid-surface with sufficient accuracy. However, as known from classical laminate theory, the in-plane stresses are accurately captured.

***layered***
A more refined discretisation can be achieved by using the knot-insertion technique described in Section 2.1.2. By inserting knots with multiplicity $p = 2$ at the coordinates corresponding to the ply interfaces, a *layered* configuration is obtained, see Figure 2.6b. Continuing with our example from above, the knot vector now takes the form $\mathbf{\Xi} = [-1, -1,\ -1,\ -1/3,\ -1/3,\ 1/3,\ 1/3,\ 1,\ 1,\ 1]$. This configuration has a much more refined through thickness discretisation, and can therefore accurately predict the through-thickness quantities such as the transverse stress. However, a consequence of this is that the *layered* state is much more computationally demanding compared to the *lumped* state.

***discontinuous***
A final configuration can be obtained by inserting a third knot into the knot vector at the coordinates where we want to model ply separation. This state is denoted the *discontinuous* state, and is exemplified in Figure 2.6c where the knot vector now takes the form $\mathbf{\Xi} = [-1, -1,\ -1,\ -1/3,\ -1/3,\ 1/3,\ 1/3,\ 1/3,\ 1,\ 1,\ 1]$. Furthermore, cohesive zone elements are used in this configuration to simulate the delamination process.

The three configurations presented above (*lumped*, *layered* and *discontinuous*) can now be used to adaptively refine the model. The model is initiated with control points in a *lumped* configuration, and then progressively refined as damage is detected and propagated. In this manner, a combination of an ELS and LW modelling approach is achieved, which will lower the total computational effort of the model.

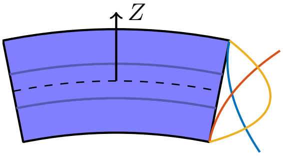


**(a)** *lumped* state

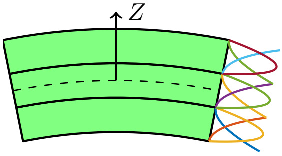


**(b)** *layered* state

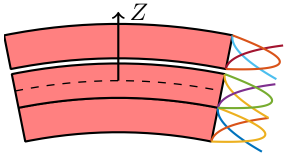


**(c)** *discontinuous* state

**Figure 2.6:** The three configurations considered in this work, denoted *lumped*, *layered* and *discontinuous*. The knot vectors, $\Xi$, are, a) $[-1, -1, -1, +1, +1, +1]$ b) $\left[-1, -1, -1, -\frac{1}{3}, -\frac{1}{3}, +\frac{1}{3}, +\frac{1}{3}, +1, +1, +1\right]$ and c) $\left[-1, -1, -1, -\frac{1}{3}, -\frac{1}{3}, +\frac{1}{3}, +\frac{1}{3}, +\frac{1}{3}, +1, +1, +1\right]$.

### 2.2.3 Stress recovery

It was previously mentioned that the coarse out-of-plane discretisation in *lumped* elements leads to poor prediction of the out-of-plane transverse stresses. In order to improve the transverse stress prediction, a method known as stress recovery has been used [17], [18]. The main idea of the stress recovery method is to use the equilibrium equations together with the gradients of the in-plane stresses to recover the transverse stresses.

The stress recovery method is at this point a relatively established method for improving the stress predictions in ESL models, and has been shown to be effective for flat plates and shells by several authors, see e.g. Främby et al. [9]. In recent years, the method has also been extended to curved geometries, see e.g. Daniel et al. [19] and Patton et al. [20].

In this thesis we use the stress recovery formulation derived in Daniel et al., for curved geometries. Since our shell element is formulated in an isogeometric framework, we obtain some interesting advantages compared to shells formulated with standard finite elements. First, the higher continuity of the spline functions in IGA results in in-plane continuity of the stress field in the domain. This means that it is possible to obtain first and second order stress gradients directly in each material point, in contrast to standard finite elements where the $C^0$ basis functions predict less accurate stress gradients. In this way, a pre-processing step for obtaining estimates of the stress gradients, as in for example Främby et al. [9], is circumvented.

A second advantage with using a stress recovery method in an isogeometric framework is that the geometry of the curved shell is represented exactly. This means that the curvature of the shell (required in the stress recovery method derived by Daniel et al.) can be computed exactly. With standard finite elements, the geometry is often meshed with piece-wise linear/flat elements with zero curvature, and therefore a patch-wise estimation of the curvature is needed here as well.

Following the works of Daniel et al., the transverse stresses for an arbitrarily curved shell can be recovered from the values and gradients of the in-plane stresses as:

$$\sigma_{13} = -\frac{1}{\lambda_1^2 \lambda_2} \int_{-t/2}^{z} \frac{\lambda_1 \lambda_2}{a_1} \sigma_{11,1} + \frac{\lambda_1^2}{a_2} \sigma_{12,2} + \frac{\lambda_1^2 a_{2,1}}{a_1 a_2} (\sigma_{11} - \sigma_{22}) + \frac{2\lambda_1 \lambda_2 a_{1,2}}{a_1 a_2} \sigma_{12} \, \mathrm{d}z + \frac{C_1}{\lambda_1^2 \lambda_2}, \quad (2.12)$$

$$\sigma_{23} = -\frac{1}{\lambda_1 \lambda_2^2} \int_{-t/2}^{z} \frac{\lambda_1 \lambda_2}{a_2} \sigma_{22,2} + \frac{\lambda_2^2}{a_1} \sigma_{12,1} + \frac{\lambda_2^2 a_{1,2}}{a_1 a_2} (\sigma_{22} - \sigma_{11}) + \frac{2\lambda_1 \lambda_2 a_{2,1}}{a_1 a_2} \sigma_{12} \, \mathrm{d}z + \frac{C_2}{\lambda_1 \lambda_2^2}, \quad (2.13)$$

$$\sigma_{33} = \frac{1}{\lambda_1 \lambda_2} \int_{-t/2}^{z} \kappa_1 \lambda_2 \sigma_{11} + \kappa_2 \lambda_1 \sigma_{22} - \frac{\lambda_1 a_{2,1}}{a_1 a_2} \sigma_{12} - \frac{\lambda_2 a_{1,2}}{a_1 a_2} \sigma_{23} \, \mathrm{d}z + \frac{C_3 + z C_4}{\lambda_1 \lambda_2}. \quad (2.14)$$

where $z$ is a coordinate in the out-of-plane directions, indices 1, 2 refer to the coordinate directions $\hat{\xi}_1$ and $\hat{\xi}_2$ oriented in the principal curvature directions of the mid-surface, and $\bullet_{,i}$ denotes derivative with respect to $\hat{\xi}_i$. The factors $a_\alpha, \alpha = 1, 2$ and $\lambda_i, i = 1, 2, 3$ are defined as:

$$\lambda_i = 1 + \kappa_i z \qquad a_\alpha = \sqrt{\bar{\mathbf{g}}_\alpha \cdot \bar{\mathbf{g}}_\alpha} \quad \text{with} \quad \alpha = 1, 2 \qquad (2.15)$$

where $\kappa_i$ are the curvature in each principal curvature direction, and $\bar{\mathbf{g}}$ are tangent vectors of the mid-surface (covariant base vectors). Furthermore, $C_1$-$C_4$ are constants arising from the integration over the shell thickness.

A recovery of the out-of-plane stresses for elements in a *lumped* configuration using Equations (2.12)-(2.14) is performed in each time-step. These stresses are then used to determine if a refinement of the element should be performed, a process which is described in the next section.

### 2.2.4 Refinement criteria

An important aspect of any adaptive method is to decide when a kinematical refinement of the model should be made. In this thesis, we follow the works by Främby et al. [9], where two refinement criteria are proposed. The first criterion is used to determine when a new delamination zone should be inserted. The criterion is based on the (recovered) stress state at the location of the interface between two adjacent plies:

$$\frac{\langle \sigma_{33} \rangle_+^2}{\sigma_{\mathrm{fn}}^2} + \frac{\sigma_{13}^2 + \sigma_{23}^2}{\sigma_{\mathrm{fs}}^2} \geq r_{\mathrm{I}}^2 \tag{2.16}$$

where $\sigma_{\mathrm{fn}}$ and $\sigma_{\mathrm{fs}}$ are the interlaminar normal and shear strengths, respectively. The Macaulay brackets $\langle \bullet \rangle_+$ are used since compressive stresses should not propagate the crack. Note that it is important to enhance the element (either from *lumped* or *layered* to *discontinuous*) well before the quadratic failure criterion exceeds 1, such that the new cohesive zone element does not enter the damage zone immediately upon insertion.

The second refinement criterion is used to decide when the delamination zone should propagate. It is known from cohesive zone modelling that the traction profile in front the crack tip play an important role for the behaviour of the cohesive zone [21], and it is therefore important to have a number of elements in front of the cohesive zone in a *discontinuous* configuration. In each converged time-step, the damage variables in the cohesive elements around the crack front are monitored. If their damage variable exceeds a predefined value (defined by the user), a search around the element is performed where *lumped* or *layered* elements within the search radius is upgraded to a *discontinuous* state.

# CHAPTER 3

## Dissipation based path-following solver

When designing fibre reinforced composite structures, it is often important to get a good understanding of its failure behaviour in order to optimise the structural design. However, if the information about the failure process is obtained using standard incremental quasi-static solvers, it is common to encounter convergence issues. These convergence issues are typically caused by the brittle failure behaviour of the cohesive zone elements used to model the delamination process. As en example, Figure 3.1 shows a (generic) force-displacement curve from a quasi-static simulation of an end-notch-flexure test, where the brittle interface parameters causes the structure to "snap-back". This snap-back can not be traced with a displacement controlled Newton solver, meaning that valuable information about the post-peak behaviour is lost. In order to more reliably obtain converged simulations and results in quasi-static solvers, it is therefore common to use so-called path-following solvers. The core idea of path-following methods is to extend the equilibrium equations with and additional *path-following constraint*.

The use of path-following solvers to analyse mechanical systems and structures first appeared in the 1970s. Wempner [22] and Riks [23] were the first

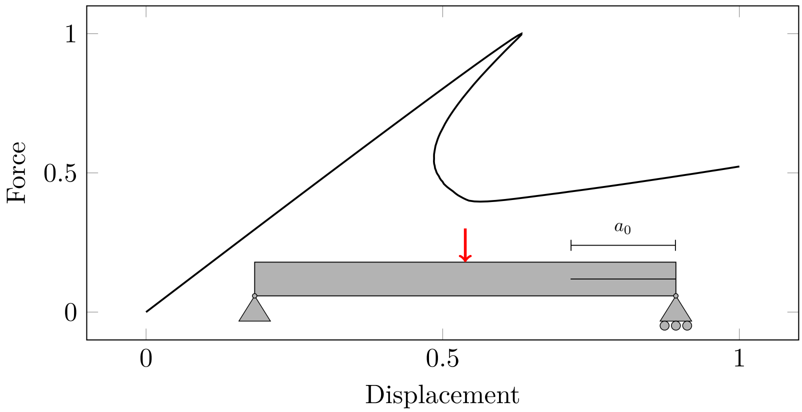


**Figure 3.1:** Illustration of snap-back behaviour when simulating an end-notch-flexure test (simply supported beam with an initial crack and applied load in the centre).

to propose a group of path-following solvers denoted as *arc-length* solvers[1], which are successful methods for analysing geometrically non-linear behaviour such as buckling. One drawback of classical arc-length solvers however, is that they are known to encounter convergence issues if they are used in simulations where local material instabilities are present. This inability to deal with material instabilities makes them unsuitable to simulate the delamination process in fibre reinforced composites.

Another group of path-following solvers that have shown to be effective in dealing with local material instabilities are dissipation-based path-following solvers. These solvers formulate the path-following constraint in terms of the dissipation rate of the active failure mechanism, and the locality of the material instability is therefore incorporated directly into the constraint. As an example, Guitierrez [24] and later Verhoosel et al. [25] derived three path-following constraints for (*i*), linear continuum elements with damage, (*ii*) linear continuum with plasticity, and (*iii*) non-linear continuum with damage. In Paper B, we propose an alternative dissipation-based path-following constraint that is based on the local dissipation rate in each material point. The benefit with this formulation is that it generalises the dissipation constraint

[1] Due to the success of arc-length solvers, they have become synonymous with path-following solvers.

to include all types of damage mechanisms.

The remainder of this chapter is organised as follows. First the equations used by path-following solvers are briefly introduced. Next, existing path-following constraints proposed in the literature are presented, followed by the path-following method constraint proposed in Paper B.

## 3.1 Fundamentals of path-following solvers

As a starting point to explain the basic relations used in path-following solvers, consider the discretised governing equations in finite element form:

$$\boldsymbol{r}(\boldsymbol{a}) = \boldsymbol{f}^{\text{int}}(\boldsymbol{a}) - \lambda\hat{\boldsymbol{f}}, \tag{3.1}$$

where $\boldsymbol{a}$ is a vector of unknown degrees of freedom (typically displacements), $\boldsymbol{r}(\boldsymbol{a})$ is the residual vector, $\boldsymbol{f}^{\text{int}}$ is the internal force vector, $\lambda$ is a load multiplier, and $\hat{\boldsymbol{f}}$ is a unit vector defining the direction of the forces. In a quasi-static setting, Equation (3.1) can be solved incrementally by controlling the load parameter $\lambda$ together with a Newton-Raphson iteration scheme. However, in path-following solvers, the load parameter is treated as an unknown variable, turning the residual into a function of two variables, $\boldsymbol{r}(\boldsymbol{a}, \lambda)$. By considering both the $\boldsymbol{a}$ and $\lambda$ as unknowns, it is possible for path-following solvers to trace the equilibrium path in the full force-displacement space.

Since an additional unknown variable has been added to the system, an additional equation has to be added as well. This equation is called the path-following constraint, $\varphi(\boldsymbol{a}, \lambda)$, and takes the general form:

$$\varphi(\boldsymbol{a}, \lambda) = 0 \tag{3.2}$$

The constraint equation $\varphi$ should be a functions of $\boldsymbol{a}$ (and possibly also $\lambda$), and be monotonically increasing.

Combining Equation (3.1) and Equation (3.1), we obtain a new system of equations,

$$\begin{bmatrix} \boldsymbol{r}(\boldsymbol{a}, \lambda) \\ \varphi(\boldsymbol{a}, \lambda) \end{bmatrix} = \begin{bmatrix} \boldsymbol{0} \\ 0 \end{bmatrix}. \tag{3.3}$$

By linearising the above equations, we can solve for both $\lambda$ and $\boldsymbol{a}$ in an incremental fashion using a Newton-Raphson scheme. The linearised system of equations take the form:

$$\begin{bmatrix} \mathrm{d}\boldsymbol{a} \\ \mathrm{d}\lambda \end{bmatrix} = \begin{bmatrix} \boldsymbol{K} & -\hat{\boldsymbol{f}} \\ \boldsymbol{h}^T & w \end{bmatrix}^{-1} \begin{bmatrix} -\boldsymbol{r} \\ -\varphi \end{bmatrix}, \tag{3.4}$$

where $\mathrm{d}\boldsymbol{a}$ and $\mathrm{d}\lambda$ are the incremental updates in a Newton-Rapson scheme, and where the Jacobian consists of the following contributions:

$$\boldsymbol{K} = \frac{\partial \boldsymbol{f}^{\mathrm{int}}}{\partial \boldsymbol{a}}, \qquad \boldsymbol{h} = \frac{\partial \varphi}{\partial \boldsymbol{a}}, \qquad w = \frac{\partial \varphi}{\partial \lambda}. \tag{3.5}$$

Note that $\boldsymbol{K}$ is the standard tangent stiffness matrix.

## 3.2 Path-following constraints

The path-following constraint used in traditional arc-length solvers, for example in Crisfield [26], takes the form:

$$\varphi(\boldsymbol{a}, \lambda) = \Delta\boldsymbol{a}^T \Delta\boldsymbol{a} + \Delta\lambda^2 - \Delta L^2 = 0, \tag{3.6}$$

where $\Delta\boldsymbol{a}$ and $\Delta\lambda$ is the incremental displacements and loads between two load steps, and $\Delta L$ is a path parameter controlling the size of the incremental step. As mentioned in the introduction to this chapter, this type of constraint is suitable for problems involving buckling, but encounters convergence issues when local material instabilities are present in the simulation.

With the aim to make path-following solver applicable to problems with material instabilities, Gutierrez [24] proposed to formulate the path-following constraint in terms of the total dissipation, $G$, of a body as

$$G = P - \dot{V}, \tag{3.7}$$

where $P$ is the external power and $\dot{V}$ are the rate of change of elastic energy. Equation (3.7) can be used to formulate path-following constraints for different damage mechanisms. As an example, a constraint for geometrically linear solids with damage can be derived by expressing the elastic energy $V$ and the external power $P$ as:

$$V = \frac{1}{2}\int_\Omega \boldsymbol{\sigma} : \boldsymbol{\varepsilon} \, \mathrm{d}\Omega = \frac{1}{2}\boldsymbol{a}^T \boldsymbol{f}^{\mathrm{int}} \tag{3.8}$$

and

$$P = \lambda \hat{\boldsymbol{f}}^T \dot{\boldsymbol{a}}, \tag{3.9}$$

where the last equalities coms from a suitable finite element discretisation, and $\Omega$ is the integration domain of the body being analysed. Using the two equations above, together with a forward Euler time discretisation, the corresponding incremental path-following constraint takes the form:

$$\varphi(\boldsymbol{a}, \lambda) = \frac{1}{2} \left( \lambda_0 \Delta \boldsymbol{a} - \Delta\lambda \boldsymbol{a}_0 \right) - \Delta\tau = 0, \tag{3.10}$$

where $\Delta\tau$ denotes the path parameter controlling the amount of dissipation allowed between two load steps, and subscript 0 denotes the previous time-step (which emanates from the use of a forward Euler time discretisation). This constraint equation was shown to give increased robustness in simulations where continuum-damage models are used.

Using the same principle as in Equation (3.7), Verhoosel et al. [25] derived two additional dissipation based constraints. For example, for geometrically non-linear solids with damage, the dissipation based constraint is:

$$\varphi(\boldsymbol{a}) = \frac{1}{2} \Delta \boldsymbol{a} \left( \lambda_0 \hat{\boldsymbol{f}} - \boldsymbol{f}_0^* \right) - \Delta\tau = 0, \quad \text{with} \qquad f_I^* = \int_\Omega \boldsymbol{E} : \boldsymbol{C} : \boldsymbol{N}_I \, \mathrm{d}\Omega \tag{3.11}$$

and where $\boldsymbol{f}_0^*$ is a global vector that needs to be assembled each load step. Furthermore, $\boldsymbol{E}$ is the Green-Lagrange strain, $\boldsymbol{C}$ is the material tangent, and $\boldsymbol{N}_I$ are basis functions. This constraint equation was shown to give increased robustness in problems with cohesive-zone models.

## 3.3 Our dissipation based path-following constraint

In Paper B, we propose to express the dissipation $G$ as an integral of the local dissipation rate in all material points, $\dot{D}$:

$$G = \int_\Omega \dot{D} \, \mathrm{d}\Omega. \tag{3.12}$$

By using a backward Euler scheme to time-discretise Equation (3.12), the path-following constraint equation $\varphi(\boldsymbol{a})$ takes the form

$$\varphi(\boldsymbol{a}) = \int_\Omega \Delta D \,\mathrm{d}\Omega - \Delta\tau = 0, \tag{3.13}$$

where $\Delta D$ is the incremental energy dissipation between two load steps. The advantage of this local formulation of the path-following constraint, is that new dissipation constraints does not need to be derived for each specific dissipation mechanisms (such as in Equation (3.10) or (3.11)), since Equation (3.13) generalises all dissipation mechanisms into one constraint equation. As an example, large strain plasticity, gradient damage and phase-field damage is also covered by Equation (3.13). Furthermore, it also allows for several simultaneous mechanisms to be considered, which is an additional improvement compared to dissipation based constraints derived for specific damage mechanisms.

With regards to implementation details, note that with the formulation in Equation (3.13), the computation of the constraint has been moved to the material routine, instead of being determined from global quantities as in for example Equation (3.10). Finally, an important aspect of the proposed path-following constraint is that an expression for $\dot{D}$ must exist. This is however often true if the material or damage model is developed in a thermodynamically consistent framework.

## 3.4 Algorithmic aspects

In this section, some algorithmic aspects of a path-following solver is discussed.

### 3.4.1 Elastic regimes of the equilibrium curve

If the gradient $\boldsymbol{h}$ in Equation (3.5) is equal to zero, i.e. no dissipation is present in the simulation, the jacobian in Equation (3.4) will be singular. This situation is encountered when the structure behaves purely elastically, for example in the beginning of the simulations or if the structure is loaded cyclically. In order to handle elastic loading, the initial steps of the simulation should be initiated with, for example, a standard force controlled or an arc-length solver. A switch to the dissipation based solver mode (Equation (3.13)) can then be made when the dissipation in the simulation exceeds some user-defined value, $\Delta\tau_{\mathrm{swtich}}$. This value should be chosen such that the solver switches to the dissipation based path-following equations before the first load-peak is reached.

Note that the simple switching algorithm outlined above will not work for complex load cases where the structure is loaded cyclically, and the structure change between dissipative and elastic behaviour throughout the simulation, in which more advanced switching techniques should be developed.

### 3.4.2 Adaptive adjustment of the path-following parameter

If the path-following parameter $\Delta\tau$ is set to a small value at the start of the simulation, each load step will become small, and the total simulation time will be long. On the other hand, if $\Delta\tau$ is set too large, there is a significant risk that the solver will diverge at load-steps where the equilibrium path is difficult to trace (such as sudden force drops). Therefore, an automatic adjustment of the path-following solver should be employed. In this thesis, the path parameter at load step $(n)$ is determined from the number of iterations, $I$, that was needed to reach convergence at previous time step $(n-1)$

$$\Delta\tau_{(n)} = \Delta\tau_{(n-1)}(\alpha)^z, \quad z = \beta(I_{(n-1)} - I_{\text{opt}}) \tag{3.14}$$

where $\alpha$ and $\beta$ are parameters that define how aggressively the path parameter should be increased/decreased, and $I_{\text{opt}}$ is the optimal number of iterations needed in the Newton-Raphson scheme. Suitable values for $\alpha$, $\beta$ and $I_{\text{opt}}$ vary depending on the type of problem, but standard values are 0.5, 0.25 and 5, respectively.

If the automatic adjustment in Equation (3.14) has increased $\Delta\tau$ to a large value near the vicinity of a sharp or sudden force drop, the Newton-Raphson iterations will likely fail to converge. In cases like these, it has been valuable to automatically half $\Delta\tau$ until convergence is reached for the current load-step. This can be expressed as:

$$\Delta\tau_{(n)} = \Delta\tau_{(n-1)} \left(\frac{1}{2}\right)^{I_{\text{F}}} \tag{3.15}$$

where $I_{\text{F}}$ is the number of non-converged attempts at the current load step.

# CHAPTER 4

## Discussion and concluding remarks

A full scale simulation of a modern fibre composite structure, where the number of layers can exceed 50 layers, will be extremely time-consuming if one wants to capture all relevant damage modes. An adaptive modelling approach, such as the one presented in this thesis, is an attempt to obtain a compromise between an efficient and accurate simulation model. The potential speed improvements, however, are heavily dependent on a number of factors. For one, if initial crack sizes are large in relation to the in-plane dimensions of the structure, a majority of the model will be initialised in a *discontinuous* state, and little speed improvements are to be gained with an adaptive model. Furthermore, if a delamination expands into a large part of the domain early on in the simulation, the same conclusion can be made. On the other hand, if a large structure is to be analysed, where the location and extension of delamination is unknown beforehand, large computational savings can be obtained.

In Paper A (and in Chapter 2 of this thesis), the developed adaptive shell element utilises the knot insertion technique from IGA, to allow for simple and flexible enhancement of the kinematics in the through-thickness direction. This facilitates more efficient simulation of delamination in fibre composites by combining the features of ESL and LW models. The isogeometric framework also provides an exact description of the geometry and smooth representation of the stress field which is beneficial for the stress recovery method.

The capabilities of the adaptive shell element are in Paper A demonstrated for the case of a doubly notched fibre composite specimen loaded in bending. From this numerical example it is shown that the through-thickness discretisation of the shell model can be refined at arbitrary interfaces, and that a speed-up factor of 1.3 is obtained (when compared to a fully resolved model). The rather small speed-up comes from the reasons discussed in the previous paragraph; the initial crack covers the half of the domain and expands into the full domain early in the simulation. It is still shown, however, that the shell element has the potential to give substantial speed gain. Note that further improvements to the efficiency of the element is possible, and is discussed in Chapter 5. Furthermore, in Paper A, it is also demonstrated that the shell element can accurately recover the through-thickness stresses for a doubly curved structure with unsymmetrical lay-up. The smooth representation of the stress field allows for element-local stress recovery, without the need for a pre-processing step for estimating the in-plane gradients.

In Section 2.2.4, two separate criteria were introduced, one for initiating new delaminations (based on the stress state of the shell), and another one for propagating the delamination zone (based on the damage state of the cohesive zone). Theoretically, the former stress-based criterion should be a good indicator for both initiation and propagation of the delamination zone. However, the shear and normal traction at the crack front is under-predicted, and can therefore not be a reliable refinement criterion to propagate the delamination zone. As such, the second criterion was introduced, and is crucial to ensure that the crack can propagate freely without interruption.

When an element in an adaptive model is refined, either from *lumped* to *layered* or *layered* to *discontinuous*, the model needs to be extended with new degrees of freedom. This will however cause changes to the internal forces, and the equilibrium state will no longer be exactly fulfilled. In a quasi-static simulation, this will result in convergence issues and an increased number of iterations will be needed to obtain convergence in the next load-step (leading to longer simulation times). A possible way to alleviate this phenomenon, was suggested by Främby et al. [9] for explicit transient simulations. Therein, they proposed to introduce a small correction force to the newly created interface nodes, and then gradually degrade the force such that the discontinuities are introduced smoothly. A similar approach could be used for quasi-static simulations.

In Paper B (and in Chapter 3 of this thesis), a path-following solver based on the dissipation of the structure is presented. The path-following constraint is formulated in terms of the integral of the local (specific) dissipation rate in a material point. An advantage of this constraint is that it encapsulates multiple dissipation based path-following constraints into one convenient formulation, which also allows the use of the solver in a wider range of problem formulations.

The robustness of the solver is demonstrated in four numerical examples in Paper B. The solver is able to trace the equilibrium path through multiple snap-back events caused by delamination in fibre composite structures. Furthermore, in the fourth numerical example of Paper B, it is shown that the proposed solver is uniquely able to trace the full equilibrium path for a load case where multiple failure mechanisms are active at once. As such, the proposed dissipation based-solver offers the possibility to robustly solve a wider range of problems previously not possible.

In Subsection 6.2 of Paper A, the adaptive isogeometric shell element and dissipation based path-following solver are combined to solve a load case consisting of a composite cantilever beam with two initial delamination cracks. It is shown that the shell element is adaptability refined as the delamination propagates through the structure, and that the full force-displacement path is traced through sharp snap-back behaviour. Furthermore, the resulting force-displacement curve shows good agreement with the experimental results. Consequently, the computational tools developed in this thesis can be used to aid the design process of fibre reinforced composite materials.

# CHAPTER 5

# Future work

In the implementation of the presented shell element, the delamination process is modelled using cohesive zone elements. A drawback of cohesive zone elements, however, is that they require a fine mesh density at the crack-front in order to accurately capture the delamination behaviour, which results in increased computational cost. A strategy to alleviate the requirement of a fine mesh density would therefore be beneficial for the efficiency of the adaptive shell element.

One strategy to alleviate the computational cost associated with fine mesh sizes required for cohesive zone elements, is to allow for adaptive mesh refinement of the in-plane direction. In this way, the adaptive shell model would only require small elements in the vicinity of the crack-front, thereby drastically reducing the computational effort. This strategy has already been investigated in the literature, see e.g. the work by Trabal et al. [27] or Lu et al. [28], where a floating node based formulation was used to adaptively refine the mesh around the crack-tip.

Another approach for addressing the computational demand of cohesive zone elements, is to use a different crack modelling technique. Here, the virtual crack closure technique (VCCT) presents an interesting alternative, since it has been shown to allow for element sizes that are larger than what is typically needed for cohesive zone elements [29]. Note however that the VCCT only works in quasi-static simulations, and needs to be further developed for use in dynamic simulations. Furthermore, many authors have also suggested improved modelling methods for cohesive zone elements. For example, Russo et al. [30] demonstrated that the use of $C^1$ continuous structural elements with rotational degrees of freedom, together with a higher order integration schemes, was able to capture the traction profile in front of the crack-tip with relatively large cohesive zone elements.

As stated in the introduction of this thesis, the heterogeneous through-thickness properties of fibre composites creates a multitude of different failure mechanisms. The main contribution of the developed shell element, however, is an adaptive framework for modelling of delamination. Although delamination plays an important role in the post-peak failure response, it is important to track all possible damage mechanisms such that the correct post-failure behaviour can be obtained. In order to use the adaptive continuum-shell element in more general load cases, it should therefore be extended with suitable models for intralaminar failure.

Regarding the dissipation based path-following solver, it would be interesting to investigate the use of the solver in other types of problems. For example, crystal-plasticity modelling or matrix materials with visco-plastic material models are both fields where snap-back might occur, and therefore could benefit from more robust solution methods.

# References


[1] *Aero QTR_04, boeing 787 from the ground up*, https://www.boeing.com/commercial/aeromagazine/articles/qtr_4_06/AERO_Q406.pdf, 2006.

[2] R. Heuss, N. Müller, W. van Sintern, D. A. Starke, and A. Tschiesner, "Lightweight, heavy impact - how carbon fiber and other lightweight materials will develop across industries and specifically in automotive.," McKinsey & Company, Tech. Rep., 2012, pp. 1–24.

[3] L. Grauers, R. Olsson, and R. Gutkin, "Energy absorption and damage mechanisms in progressive crushing of corrugated ncf laminates: Fractographic analysis," *Composite Structures*, vol. 110, pp. 110–117, 2014.

[4] D. Hull, "A unified approach to progressive crushing of fibre-reinforced composite tubes," *Composites Science and Technology*, vol. 40, no. 4, pp. 377–421, 1991.

[5] P. Feraboli, B. Wade, F. Deleo, M. Rassaian, M. Higgins, and A. Byar, "Ls-dyna mat54 modeling of the axial crushing of a composite tape sinusoidal specimen," *Composites Part A: Applied Science and Manufacturing*, vol. 42, no. 11, pp. 1809–1825, 2011.

[6] S. Costa, T. Bru, R. Olsson, and A. Portugal, "Improvement and validation of a physically based model for the shear and transverse crushing of orthotropic composites," *Journal of Composite Materials*, vol. 53, no. 12, pp. 1681–1696, 2019.

[7] S. Pinho, L. Iannucci, and P. Robinson, "Physically based failure models and criteria for laminated fibre-reinforced composites with emphasis on fibre kinking. part ii: Fe implementation," *Composites Part A: Applied Science and Manufacturing*, vol. 37, no. 5, pp. 766–777, 2006.

[8] R. Larsson, "A discontinuous shell-interface element for delamination analysis of laminated composite structures," *Computer Methods in Applied Mechanics and Engineering*, vol. 193, no. 30, pp. 3173–3194, 2004, Computational Failure Mechanics.

[9] J. Främby, M. Fagerström, and J. Brouzoulis, "Adaptive modelling of delamination initiation and propagation using an equivalent single-layer shell approach," *International Journal for Numerical Methods in Engineering*, vol. 112, no. 8, pp. 882–908, 2017.

[10] M. McElroy, "Use of an enriched shell finite element to simulate delamination-migration in a composite laminate," *Composite Structures*, vol. 167, pp. 88–95, 2017.

[11] C. Adams, M. Fagerström, and J. J. C. Remmers, "Efficient modelling of delamination growth using adaptive isogeometric continuum shell elements," *Computational Mechanics*, vol. 65, no. 1, pp. 99–117, Jan. 2020.

[12] S. Hosseini, J. J. C. Remmers, C. V. Verhoosel, and R. de Borst, "An isogeometric continuum shell element for non-linear analysis," *Computer Methods in Applied Mechanics and Engineering*, vol. 271, pp. 1–22, Apr. 2014.

[13] T. Hughes, J. Cottrell, and Y. Bazilevs, "Isogeometric analysis: Cad, finite elements, nurbs, exact geometry and mesh refinement," *Computer Methods in Applied Mechanics and Engineering*, vol. 194, no. 39, pp. 4135–4195, 2005.

[14] Y. Bazilevs, V. Calo, J. Cottrell, *et al.*, "Isogeometric analysis using t-splines," *Computer Methods in Applied Mechanics and Engineering*, vol. 199, no. 5, pp. 229–263, 2010, Computational Geometry and Analysis.

[15] L. Leidinger, M. Breitenberger, A. Bauer, *et al.*, "Explicit dynamic isogeometric b-rep analysis of penalty-coupled trimmed nurbs shells," *Computer Methods in Applied Mechanics and Engineering*, vol. 351, pp. 891–927, 2019.

[16] L. F. Leidinger, M. Breitenberger, A. M. Bauer, *et al.*, “Explicit isogeometric b-rep analysis on trimmed nurbs-based multi-patch cad models in ls-dyna,” in *Proceedings of 12th European LS-DYNA Conference*, Germany, Koblenz, 2019.

[17] R. Rolfes, K. Rohwer, and M. Ballerstaedt, “Efficient linear transverse normal stress analysis of layered composite plates,” *Computers & Structures*, vol. 68, no. 6, pp. 643–652, 1998.

[18] R. Rolfes and K. Rohwer, “Improved transverse shear stresses in composite finite elements based on first order shear deformation theory,” *International Journal for Numerical Methods in Engineering*, vol. 40, no. 1, pp. 51–60, 1997.

[19] P. M. Daniel, J. Främby, M. Fagerström, and P. Maimí, “Complete transverse stress recovery model for linear shell elements in arbitrarily curved laminates,” *Composite Structures*, vol. 252, p. 112 675, 2020.

[20] A. Patton, P. Antolín, J. Kiendl, and A. Reali, “Efficient equilibrium-based stress recovery for isogeometric laminated curved structures,” *Composite Structures*, vol. 272, p. 113 975, Sep. 2021.

[21] A. Turon, C. Dávila, P. Camanho, and J. Costa, “An engineering solution for mesh size effects in the simulation of delamination using cohesive zone models,” *Engineering Fracture Mechanics*, vol. 74, no. 10, pp. 1665–1682, 2007.

[22] G. A. Wempner, “Discrete approximations related to nonlinear theories of solids,” *International Journal of Solids and Structures*, vol. 7, no. 11, pp. 1581–1599, 1971.

[23] E. Riks, “The Application of Newton’s Method to the Problem of Elastic Stability,” *Journal of Applied Mechanics*, vol. 39, no. 4, pp. 1060–1065, Dec. 1972.

[24] M. A. Gutiérrez, “Energy release control for numerical simulations of failure in quasi-brittle solids,” *Communications in Numerical Methods in Engineering*, vol. 20, no. 1, pp. 19–29, Jan. 2004.

[25] C. V. Verhoosel, J. J. Remmers, and M. A. Gutiérrez, “A dissipation-based arc-length method for robust simulation of brittle and ductile failure,” *International Journal for Numerical Methods in Engineering*, vol. 77, no. 9, pp. 1290–1321, Feb. 2009.

[26] M. Crisfield, "A fast incremental/iterative solution procedure that handles "snap-through"," *Computers and Structures*, vol. 13, no. 1-3, pp. 55–62, Jun. 1981.

[27] G. G. Trabal, B. L. V. Bak, B. Chen, and E. Lindgaard, "An adaptive floating node based formulation for the analysis of multiple delaminations under quasi-static loading," *Composites Part A: Applied Science and Manufacturing*, vol. 156, p. 106 846, 2022.

[28] X. Lu, B. Chen, V. Tan, and T. Tay, "Adaptive floating node method for modelling cohesive fracture of composite materials," *Engineering Fracture Mechanics*, vol. 194, pp. 240–261, 2018.

[29] M. W. McElroy, "An enriched shell finite element for progressive damage simulation in composite laminates," NASA/TP-2016-219211, Tech. Rep., 2016.

[30] R. Russo and B. Chen, "Overcoming the cohesive zone limit in composites delamination: Modeling with slender structural elements and higher-order adaptive integration," *International Journal for Numerical Methods in Engineering*, vol. 121, no. 24, pp. 5511–5545, 2020.